Phosphorus Radicals

Deutsche Ausgabe: DOI: 10.1002/ange.201502737
Internationale Ausgabe: DOI: 10.1002/anie.201502737

Synthesis and EPR/UV/Vis-NIR Spectroelectrochemical Investigation of a Persistent Phosphanyl Radical Dication

*Kai Schwedtmann, Stephen Schulz, Felix Hennersdorf, Thomas Strassner, Evgenia Dmitrieva, and Jan J. Weigand**

Dedicated to Professor Manfred Scheer on the occasion of his 60th birthday

Abstract: *The reaction of the bis(imidazoliumyl)-substituted P^I cation [(2-Im^{Dipp})P(4-Im^{Dipp})]$^+$ (**10**$^+$) (2-Im = imidazolium-2-yl; 4-Im = imidazolium-4-yl; Dipp = 2,6-di-isopropylphenyl) with trifluoromethanesulfonic acid (HOTf) or methyl trifluoromethylsulfonate (MeOTf) yields the corresponding protonated [(2-Im^{Dipp})PH(4-Im^{Dipp})]$^{2+}$ (**11**$^{2+}$) and methylated [(2-Im^{Dipp})PMe(4-Im^{Dipp})]$^{2+}$ (**12**$^{2+}$) dications, respectively. EPR/UV/Vis-NIR spectroelectrochemical investigation of the low-coordinated P^I cation **10**$^+$ predicted a stable and "bottleable" P-centered radical dication [(2-Im^{Dipp})P(4-Im^{Dipp})]$^{2+\bullet}$ (**13**$^{2+\bullet}$). The reaction of **10**$^+$ with the nitrosyl salt NO[OTf] yields the persistent phosphanyl radical dication **13**$^{2+\bullet}$ as triflate salt in crystalline form. Quantum chemical investigation revealed an exceptional high spin density at the P atom.*

Among several bonding motifs possible for charged and uncharged P_1-centered radicals, phosphanyl radicals are particularly intriguing.[1] Such radicals feature a two-coordinate P atom in the +II oxidation state in combination with either C- (I) or N-based (II)—or a combination of both (III)—substituents L_C or L_N (Scheme 1). Especially low-coordinate P-radical species require stabilization by either bulky substituents (kinetic stabilization), and/or spin delocalization (thermodynamic stabilization).[2] However, only a few examples are known that are stable enough to be isolated in the solid state. Representative examples of isolated and structurally characterized neutral (**1**$^\bullet$–**5**$^\bullet$),[3–6] anionic (**6**$^{-\bullet}$),[7] and cationic (**7**$^{+\bullet}$, **8**$^{+\bullet}$)[8,9] derivatives are depicted in Scheme 1. The stability of the radical cations is also explained by the positive charge leading to electrostatic repulsive effects. Surprisingly, and to the best of our knowledge, no example of a phosphanyl radical dication has been reported so far, although with the isolation of radical cations of type **7**$^{+\bullet}$ and **8**$^{+\bullet}$ those species should be feasible. Thus, a dicationic radical species might be accessible by a formal exchange of the L_N substituent in cations of type **7**$^{+\bullet}$ or **8**$^{+\bullet}$ by an imidazoliumyl substituent. Recently, we reported on the high-yielding synthesis of the cationic phosphanide **10**$^+$, bearing two lone pairs of electrons at the P atom, which we obtained from the reduction of dication **9**$^{2+}$ (Scheme 2).[10] Cation **10**$^+$ is supposed to react with electrophiles such as trifluoromethanesulfonic acid (HOTf) or methyl trifluoromethylsulfonate (MeOTf) to give the respective protonated (**11**$^{2+}$) and methylated dications (**12**$^{2+}$) as triflate salts, respectively (Scheme 2). The unique combination of the C-bonded N-heterocyclic substituents (L_C) on the two-coordinate phosphorus atom in cation **10**$^+$ makes it an excellent substrate for the synthesis of the hitherto unknown phosphanyl radical dication **13**$^{2+\bullet}$ (Scheme 2).

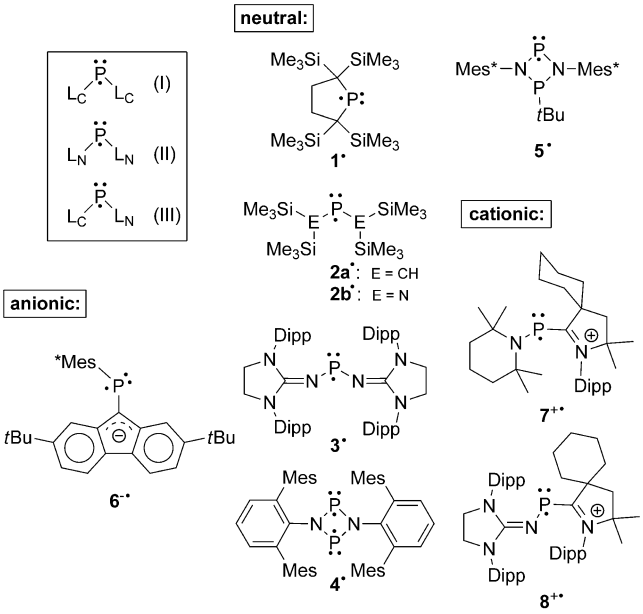

Scheme 1. Structurally characterized phosphanyl radicals.

Reacting **10**$^+$ with HOTf or MeOTf in CH_2Cl_2 gives the expected dications **11**$^{2+}$ (88%) and **12**$^{2+}$ (83%) as triflate salts in very good yield (Scheme 2).[11] Both compounds are obtained as colorless, moisture-sensitive crystalline material.

[*] K. Schwedtmann, S. Schulz, F. Hennersdorf, Prof. Dr. J. J. Weigand
TU Dresden, Professur für Anorganische Molekülchemie
01062 Dresden (Germany)
E-mail: jan.weigand@tu-dresden.de
Prof. Dr. T. Strassner
TU Dresden, Professur für Physikalische Organische Chemie
01062 Dresden (Germany)
Dr. E. Dmitrieva
Leibniz-Institut für Festkörper- und
Werkstoffforschung Dresden, 01069 Dresden (Germany)

Supporting information for this article is available on the WWW under http://dx.doi.org/10.1002/anie.201502737.

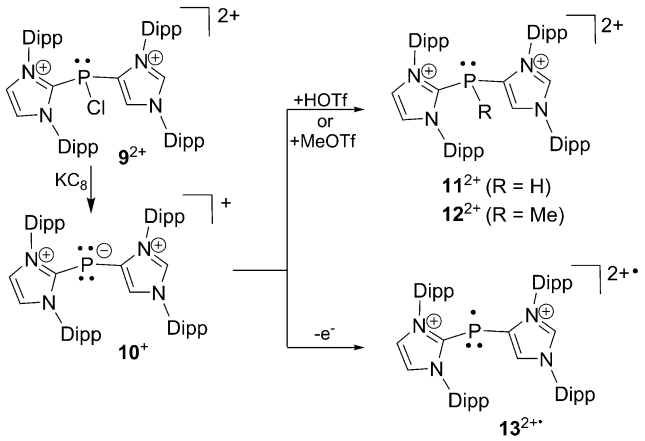

Scheme 2. Reaction of cation $\mathbf{10}^+$ with electrophiles (HOTf, MeOTf) to dications $\mathbf{11}^{2+}$ and $\mathbf{12}^{2+}$ and oxidation to radical dication $\mathbf{13}^{2+\bullet}$.

The ^{31}P NMR spectrum of the purified compound $\mathbf{11}[OTf]_2$ displays a doublet resonance at $\delta = -117.9$ ppm exhibiting an expected $^1J_{PH}$ coupling constant of 251 Hz.[12] For compound $\mathbf{12}[OTf]_2$ a quartet resonance is observed at $\delta = -54.4$ ppm with a $^2J_{PH}$ coupling constant of 9 Hz consistent with a methyl group attached to the three-coordinate P atom. Suitable crystals for X-ray investigation were obtained for compound $\mathbf{11}[OTf]_2$ and the molecular arrangement of cation $\mathbf{11}^{2+}$ is depicted in Figure 1a. As expected,

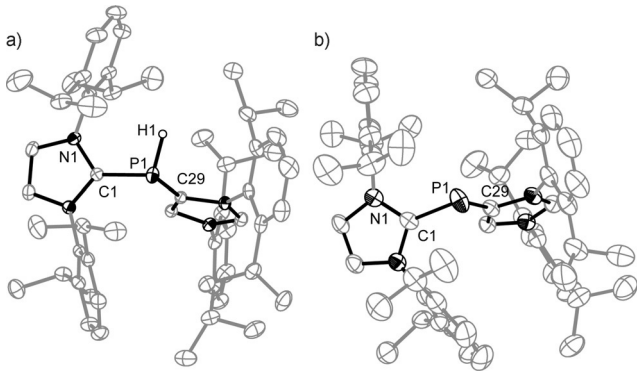

Figure 1. a) Molecular structure of dication $\mathbf{11}^{2+}$. Selected bond lengths (Å) and angles (°): P1–C1 1.813(3), P1–C29 1.821(2); C1–P1–C29 101.82(10), C1–P1–H1 94.5(14), C29–P1–H1 102.1(14); torsion angle: C29–P1–C1–N1 113.5(2). b) Molecular structure of radical dication $\mathbf{13}^{2+\bullet}$. P1–C1 1.808(4), P1–C29 1.800(4); C1–P1–C29 102.15(16); torsion angle: C29–P1–C1–N1 114.8(3). Solvent molecules anions and carbon bonded hydrogen atoms are omitted for clarity, and thermal ellipsoids are displayed at 50% probability (153 K).

cation $\mathbf{11}^{2+}$ displays a distorted trigonal pyramidal bonding environment around the P atom. The P–C bond lengths (P1–C1 1.813(3) Å, P1–C29 1.821(2) Å) are in the expected range and comparable to those observed for dication $\mathbf{9}^{2+}$ (P1–C1 1.838(3) Å, P1–C29 1.820(2) Å).[10] In particular, the elongation of the P1–C1 bond length compared to that of $\mathbf{10}^+$ (P1–C1 1.773(3) Å) is consistent with a lesser degree of π-bonding between C1 and P1. The C1–P1–C29 angle (101.82(10)°) is slightly narrower compared to C1–P1–C29 (109.2(1)°) of $\mathbf{10}^+$, but there is a dramatic difference in the torsion angles for the two cations ($\mathbf{11}^{2+}$: C29–P1–C1–N1 113.5(2)°; $\mathbf{10}^+$: C29–P1–C1–N1 170.80(16)°), showing that the imidazoliumyl substituents are substantially twisted in the dicationic structure of $\mathbf{11}^{2+}$.

Anticipating an interesting reduction/oxidation behavior of cation $\mathbf{10}^+$ (see Scheme 3) we performed an EPR/UV/Vis-

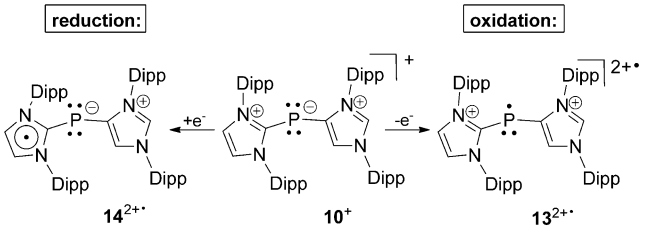

Scheme 3. Electrochemical reduction of cation $\mathbf{10}^+$ to unstable neutral radical $\mathbf{14}^\bullet$ and oxidation to radical dication $\mathbf{13}^{2+\bullet}$.

NIR spectroelectrochemical[13] investigation to elucidate the possibility for the preparation of stable radicals. The cyclic voltammogram of a solution of $\mathbf{10}[OTf]$ in THF/nBu$_4$N[OTf] (0.1 M) shows one reversible oxidation at $E_{1/2} = 0.22$ V (vs. $E_{1/2}$ (Fc/Fc$^+$)) and one irreversible reduction peak at $E_p = -3.06$ V (vs. $E_{1/2}$(Fc/Fc$^+$); Figure 3a). Peak parameters of the oxidation ($\mathbf{10}^+ \rightarrow \mathbf{13}^{2+\bullet}$) to radical dication $\mathbf{13}^{2+\bullet}$ at given scan rate and their behavior at higher scan rates indicate a reversible electrochemical oxidation.

In contrast to the oxidation the peak shape of the reduction to neutral radical $\mathbf{14}^\bullet$ is assigned to an electrochemical irreversible reaction or a follow-up reaction (see Figure S3 in the Supporting Information).[14] The in situ reflective measurement[15] (Figure S5) of the UV/Vis-NIR spectra of the electrode surface during a cyclic voltammetry (CV) measurement (Figure 2, Vis-CV Figure S6) reveal further insights into the formation of red-colored radical species. The Vis part of the UV/Vis-NIR spectra (x axis) during three cycles of CV measurements of $\mathbf{10}^+$ is shown and correlated to the time (left y axis) and the potential (right y axis; Figure 2). When the oxidation potential reaches a value of $E > 0.22$ V, radical dication $\mathbf{13}^{2+\bullet}$ is formed and its characteristic band at 487 nm can be observed (spectrum at this potential: orange curve, top). Afterwards, radical dication $\mathbf{13}^{2+\bullet}$ is reduced back to cation $\mathbf{10}^+$ (negative peak, right y axis). At comparably strong negative potentials ($E < -3.06$ V) $\mathbf{10}^+$ is reduced to neutral radical $\mathbf{14}^\bullet$ (spectrum at this potential: green curve, top). An appearance of the assigned band at 451 nm (see Figure S6) and the disappearance without a peak at the corresponding potential in the current curve of the CV measurement (Figure 3a) can be attributed to a low stability of neutral radical $\mathbf{14}^\bullet$. A differentiation between an irreversible electrochemical process and a follow-up reaction is given by CV measurement at high scan rates, where the oxidation peak of $\mathbf{14}^\bullet$ is observed (see Figure S4).[16] A more preparative evidence on the stability of radical dication $\mathbf{13}^{2+\bullet}$ and instability of $\mathbf{14}^\bullet$ is given by EPR/UV/Vis-NIR spectro-electrochemistry in thin-layer cells[17,18]

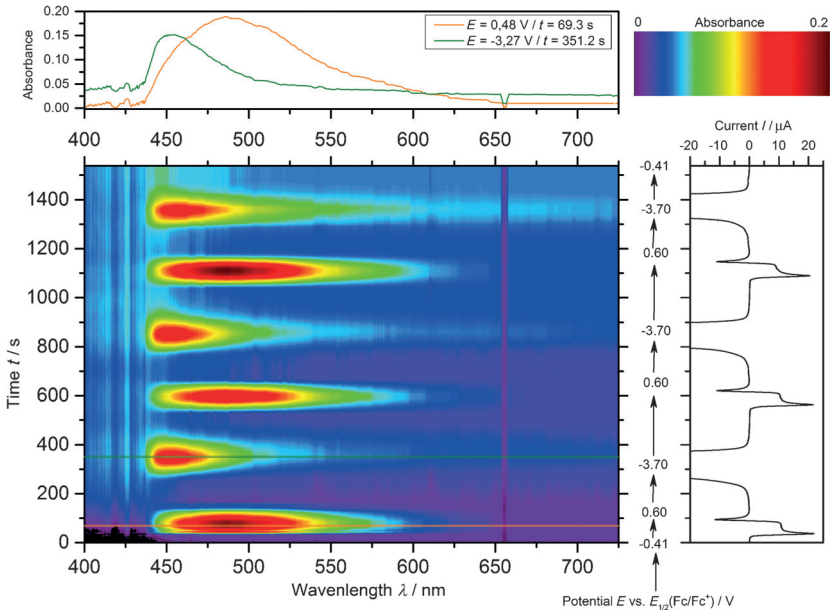

Figure 2. In situ reflective UV/Vis-NIR spectroelectrochemical measurement of a Pt disc electrode surface of a $CH_2Cl_2/nBu_4N[OTf]$ (0.1 M) solution of **10**[OTf] (1.3×10^{-3} M) during a cyclic voltammogram ($\nu = 15$ mV s^{-1}). Corresponding Vis spectra of formed $\mathbf{13}^{2+\bullet}$ (orange curve, top), radical $\mathbf{14}^{\bullet}$ (green curve, top) and current time–potential curve (right).

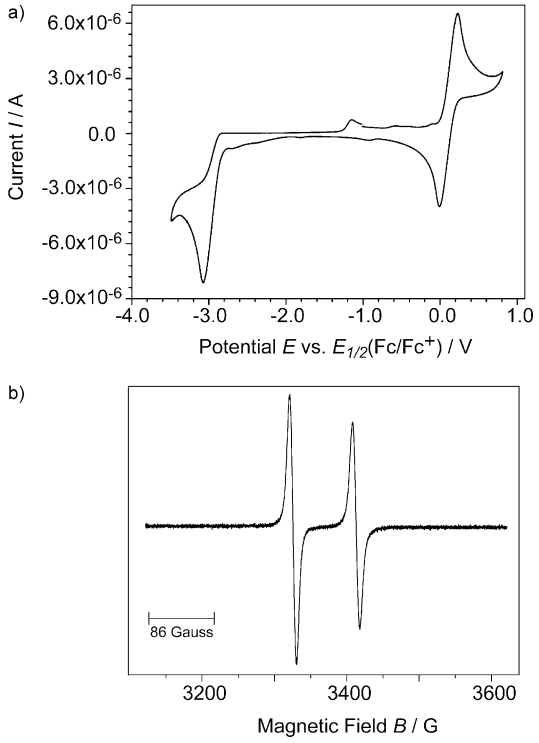

Figure 3. a) Cyclic voltammorgram of a THF/$nBu_4N[OTf]$ solution of **10**[OTf] at a glassy carbon disc electrode. b) EPR spectrum of **13**$[OTf]_2$ in o-$C_6H_4F_2$ at ambient temperature.

with complete conversion of the substrate $\mathbf{10}^{+}$. The UV/Vis-NIR-CV measurements show UV/Vis absorptions at 248, 287, 323, 395, and 487 nm for radical dication $\mathbf{13}^{2+\bullet}$ accompanied by the disappearance of the absorption at 418 nm for $\mathbf{10}^{+}$ (see Figures S7 and S8). The potential dependencies of the emerging absorption bands and that of the EPR signal are in good agreement (see Figure S9). Contrariwise, no absorptions in the UV/Vis spectra can be observed for the reductive reaction, even at low potentials, indicating the aforementioned low stability of $\mathbf{14}^{\bullet}$. This result in combination with high-speed CV measurements (see Figure S4), in which the reduction process shows a more reversible character, give evidence for a chemical follow-up reaction of radical $\mathbf{14}^{\bullet}$. Quantum chemical calculations of $\mathbf{14}^{\bullet}$ have shown that the spin density is to a large extend located at the C2-bound imidazolyl ring (80%; see section S3.7 in the Supporting Information). The results of the spectroelectrochemical investigations forecast the preparative accessibility of stable radical dication $\mathbf{13}^{2+\bullet}$. Thus, reacting **10**[OTf] with one equivalent of nitrosyl triflate (NO[OTf])[19] in THF at −78 °C leads upon warming to ambient temperature to a deep-red suspension. After workup, the extremely air- and moisture sensitive P-centered radical dication $\mathbf{13}^{2+\bullet}$ was isolated as red powder in good yield as triflate salt (73%, Scheme 4). The room temperature EPR

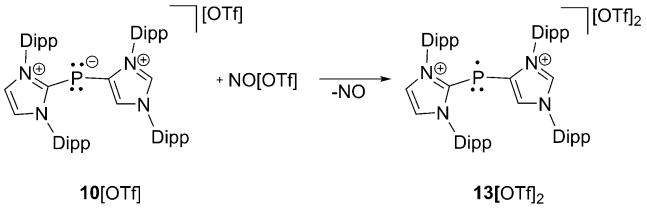

Scheme 4. Oxidation of **10**[OTf] with NO[OTf] to **13**$[OTf]_2$ in THF from −78 °C to RT.

spectrum of **13**$[OTf]_2$ in o-difluorobenzene displays a doublet ($g = 2.006$) due to a large hyperfine coupling constant with the phosphorus nucleus [$a(^{31}P) = 86$ G] (Figure 3b). This hyperfine coupling constant is comparable to those observed for other phosphanyl radicals[3–9] with a typical range of $a(^{31}P) =$ 42–99 G. Interestingly, no hyperfine coupling is observed to the ^{14}N atoms, indicating that the singly occupied molecular orbital (SOMO) is barely delocalized over the π-conjugated substituents but located primarily at the P atom. Deep-red single crystals, suitable for X-ray diffraction study, were obtained by slow diffusion of n-pentane into a o-difluorobenzene solution of **13**$[OTf]_2$ at −35 °C.

The molecular structure (Figure 1b) of radical dication $\mathbf{13}^{2+\bullet}$ reveals a bent bonding environment at the P atom with a C1–P–C29 angle of 102.15(16)°. Similar to the molecular structure of dication $\mathbf{11}^{2+}$ the imidazoliumyl substituents are strongly twisted ($\mathbf{13}^{2+\bullet}$: C29–P1–C1–N1 114.8(3)°). The P1–C1 and P1–C29 bond lengths (1.808(4) Å, 1.800(4) Å) are

elongated, compared to $\mathbf{10}^{+}$, also showing a lesser degree of π bonding between P1 and C1. However, compared to dication $\mathbf{11}^{2+}$ the P–C bond lengths in $\mathbf{13}^{2+\bullet}$ are slightly shorter, indicating a partial delocalization of the single electron, which is also shown by the quantum chemical calculations, performed using the Gaussian09 program suite.[11,20] The density functional theory (DFT) hybrid models B3LYP[21] and M06[22] were used together with the 6-31G(d) basis set[23] for geometry optimizations. The spin density has been calculated by different methods. Both agree that it is largely centered on the P atom and also that it is around 80% (B3LYP: 79%; M06: 81%), consistent with the considerably high spin localization on the P atom observed by EPR spectroscopy. Single-point calculations with different methods based on the B3LYP optimized geometry came to the same results or gave even higher spin densities.[11] Figure 4

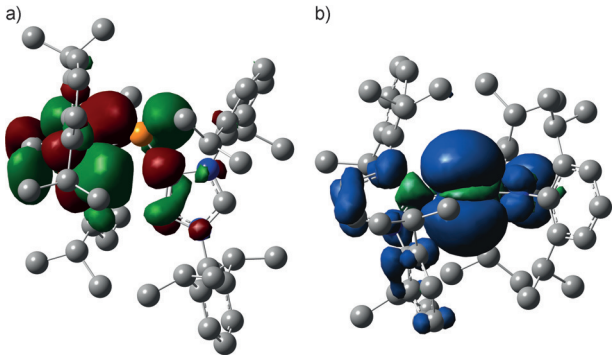

Figure 4. a) Calculated SOMO and b) spin density distribution of radical dication $\mathbf{13}^{2+\bullet}$ (B3LYP/6-31G(d); hydrogen atoms are omitted for clarity).

shows the calculated SOMO (left) illustrating that it has primarily p-orbital character and the spin density distribution from the fully optimized B3LYP/6-31G(d) structure of radical dication $\mathbf{13}^{2+\bullet}$ (right). The calculated geometrical parameters (C1–P1–C29 104.9°; P1–C1 1.853 Å, P1–C29 1.805 Å; C29–P1–C1–N1 107.8°) are in good agreement with the data from the solid-state structure although there are slight differences within the two imidazolium ring systems. The NBO analysis yielded Wiberg bond indices of 1.0252 and 0.9348 for the P1–C29 and P1–C1 bonds, respectively. The natural bond orbital (NBO) bond order was calculated as 0.8696 (P1–C29) and 0.8197 (P1–C1). The calculated Mulliken and NPA charges are given in the supporting information (see S3.11, SI). The aforementioned results reveal the stability of radical dication $\mathbf{13}^{2+\bullet}$ is not only contributed by a thermodynamic stabilization (conjugated π system) but more by kinetic stabilization (bulky substituents, charge repulsion).

In summary, we illustrated that the two-coordinate P^{I} cation ($\mathbf{10}^{+}$) readily reacts with HOTf or MeOTf to give the corresponding protonated ($\mathbf{11}^{2+}$) and methylated ($\mathbf{12}^{2+}$) dications, respectively. In-depth EPR/UV/Vis-NIR spectroelectrochemical investigations of $\mathbf{10}^{+}$ revealed two radical species $\mathbf{14}^{\bullet}$, by electrochemical reduction, and $\mathbf{13}^{2+\bullet}$, by electrochemical oxidation, whereat the latter was predicted to be persistent in solution and the solid state. The reaction of $\mathbf{10}^{+}$ with nitrosyl triflate leads to the formation of the remarkable and stable phosphanyl radical dication $\mathbf{13}^{2+\bullet}$ showing a high spin density at the P atom. This work shows the accessibility of a stable phosphanyl radical dication, namely $\mathbf{13}^{2+\bullet}$, and extends the already existing set of intriguing phosphanyl radical species (Scheme 1).

Acknowledgements

This work was supported by the Fonds der Chemischen Industrie (FCI, Kekulé scholarship for F.H.) and the German Science Foundation (DFG, grant number WE 4621/2-1) and the ERC (grant number SynPhos 307616). We thank the Center for Information Services and High Performance Computing (ZIH) for the generous allocation of computation time.

Keywords: dications · EPR spectroscopy · phosphorus · radicals · spectroelectrochemistry

How to cite: *Angew. Chem. Int. Ed.* **2015**, *54*, 11054–11058
Angew. Chem. **2015**, *127*, 11206–11210

[1] For reviews see: a) A. Armstrong, T. Chivers, R. T. Boere, *ACS Symp. Ser.* **2006**, *917*, 66; b) S. Marque, P. Tordo, *Top. Curr. Chem.* **2005**, *250*, 43; c) P. P. Power, *Chem. Rev.* **2003**, *103*, 789; d) M. Geoffroy, *Recent Res. Dev. Phys. Chem. Solids* **1998**, *2*, 311; e) M. D. Caleb, M. Soleilhavoup, G. Bertrand, *Chem. Sci.* **2013**, *4*, 3020, and references therein.

[2] a) P. Agarwal, N. A. Piro, K. Meyer, P. Muller, C. C. Cummins, *Angew. Chem. Int. Ed.* **2007**, *46*, 3111; *Angew. Chem.* **2007**, *119*, 3171; b) A. Armstrong, T. Chivers, M. Parvez, R. T. Boere, *Angew. Chem. Int. Ed.* **2004**, *43*, 502; *Angew. Chem.* **2004**, *116*, 508; c) S. Ito, M. Kikuchi, M. Yoshifuji, A. J. Arduengo III, T. A. Konovalova, L. D. Kispert, *Angew. Chem. Int. Ed.* **2006**, *45*, 4341; *Angew. Chem.* **2006**, *118*, 4447; d) M. Scheer, C. Kuntz, M. Stubenhofer, M. Linseis, R. F. Winter, M. Sierka, *Angew. Chem. Int. Ed.* **2009**, *48*, 2600; *Angew. Chem.* **2009**, *121*, 2638.

[3] S. Ishida, F. Hirakawa, T. Iwamoto, *J. Am. Chem. Soc.* **2011**, *133*, 12968.

[4] a) S. L. Hinchley, C. A. Morrison, D. W. H. Rankin, C. L. B. Macdonald, R. J. Wiacek, A. H. Cowley, M. F. Lappert, G. Gundersen, J. A. C. Clyburne, P. P. Power, *Chem. Commun.* **2000**, 2045; b) S. L. Hinchley, C. A. Morrison, D. W. H. Rankin, C. L. B. Macdonald, R. J. Wiacek, A. Voigt, A. H. Cowley, M. F. Lappert, G. Gundersen, J. A. C. Clyburne, P. P. Power, *J. Am. Chem. Soc.* **2001**, *123*, 9045; c) J. P. Bezombes, K. B. Borisenko, P. B. Hitchcock, M. F. Lappert, J. E. Nycz, D. W. H. Rankin, H. E. Robertson, *Dalton Trans.* **2004**, 1980.

[5] O. Back, B. Donnadieu, M. von Hopffgarten, S. Klein, R. Tonner, G. Frenking, G. Bertrand, *Chem. Sci.* **2011**, *2*, 858.

[6] T. Beweries, R. Kuzora, U. Rosenthal, A. Schulz, A. Villinger, *Angew. Chem. Int. Ed.* **2011**, *50*, 8974; *Angew. Chem.* **2011**, *123*, 9136.

[7] X. Pan, X. Wang, Y. Zhao, Y. Sui, X. Wang, *J. Am. Chem. Soc.* **2014**, *136*, 9834.

[8] O. Back, M. A. Celik, G. Frenking, M. Melaimi, B. Donnadieu, G. Bertrand, *J. Am. Chem. Soc.* **2010**, *132*, 10262.

[9] R. Kinjo, B. Donnadieu, G. Bertrand, *Angew. Chem. Int. Ed.* **2010**, *49*, 5930; *Angew. Chem.* **2010**, *122*, 6066.

[10] K. Schwedtmann, M. H. Holthausen, K.-O. Feldmann, J. J. Weigand, *Angew. Chem. Int. Ed.* **2013**, *52*, 14204; *Angew. Chem.* **2013**, *125*, 14454.

[11] See supporting information for further details.
[12] O. Kühl, *Phosphorus-31 NMR Spectroscopy*, Springer, Berlin, **2008**.
[13] a) W. Kaim, J. Fiedler, *Chem. Soc. Rev.* **2009**, *38*, 3373; b) W. Kaim, A. Klein, *Spectroelectrochemistry*, Royal Society of Chemistry, Cambridge, **2008**, and references therein; c) A. Petr, L. Dunsch, A. Neudeck, *J. Electroanal. Chem.* **1996**, *412*, 153; d) L. Dunsch, *J. Electroanal. Chem.* **1975**, *61*, 61.
[14] J. Heinze, *Angew. Chem. Int. Ed. Engl.* **1984**, *23*, 831; *Angew. Chem.* **1984**, *96*, 823.
[15] a) U. Schroeder, F. Scholz, *J. Solid State Electrochem.* **1997**, *1*, 62; b) F. Scholz, *Electroanalytical Methods*, Springer, Berlin, **2002**.
[16] a) J. M. Saveant, *Electrochim. Acta* **1967**, *12*, 999; b) R. S. Nicholson, I. Shain, *Anal. Chem.* **1964**, *36*, 706.
[17] J. Niu, S. Dong, *Rev. Anal. Chem.* **1996**, *15*, 1.
[18] a) R. W. Murray, W. R. Heinemann, G. W. O'Dom, *Anal. Chem.* **1967**, *39*, 1666; b) T. P. DeAgelis, W. R. Heineman, *J. Chem. Educ.* **1967**, *44*, 594.
[19] The synthesis of nitrosyl triflate was carried out according to a literature procedure: R. Weiss, K.-G. Wagner, *Chem. Ber.* **1984**, *117*, 1973.
[20] M. L. Frisch; Gaussian 09, Revision A.02, Gaussian, Inc., Wallingford CT, **2009**; for a complete list of authors see the Supporting Information.
[21] a) A. D. Becke, *J. Chem. Phys.* **1993**, *98*, 5648; b) C. Lee, W. Yang, R. G. Parr, *Phys. Rev. B* **1988**, *37*, 785; c) P. J. Stephens, E. J. Devlin, C. F. Chabalowski, M. J. Frisch, *J. Phys. Chem.* **1994**, *98*, 11623; d) S. H. Vosko, L. Wilk, M. Nusair, *Can. J. Phys.* **1980**, *58*, 1200.
[22] a) Y. Zhao, D. G. Truhlar, *Theor. Chem. Acc.* **2008**, *119*, 525; b) Y. Zhao, D. G. Truhlar, *Theor. Chem. Acc.* **2008**, *120*, 215.
[23] a) W. J. Hehre, R. Ditchfield, J. A. Pople, *J. Chem. Phys.* **1980**, *72 – 73*, 2257; b) M. M. Francl, W. J. Pietro, W. J. Hehre, J. S. Binkley, M. S. Gordon, D. J. DeFrees, J. A. Pople, *J. Chem. Phys.* **1982**, *77*, 3654; c) R. C. Binning, Jr., L. A. Curtiss, *J. Comput. Chem.* **1990**, *11*, 1206.

Received: March 24, 2015
Published online: July 31, 2015

